Desalination and Water Treatment
www.deswater.com
doi: 10.1080/19443994.2014.995714

57 (2016) 4659–4670
February

Taylor & Francis
Taylor & Francis Group

Direct Blue 71 removal by electrocoagulation sludge recycling in photo-Fenton process: response surface modeling and optimization

Mahsa Moradi[a], Akbar Eslami[a], Farshid Ghanbari[b,*]

[a]*Department of Environmental Health Engineering, School of Public Health, Shahid Beheshti University of Medical Sciences, Tehran, Iran, Tel. +98 9126907929; email: Moradi.env@gmail.com (M. Moradi), Tel. +98 9123410393; email: aeslami@sbmu.ac.ir (A. Eslami)*
[b]*Department of Environmental Health Engineering, School of Public Health, Ahvaz Jundishapur University of Medical Sciences, Ahvaz 61357-15794, Iran, Tel. +98 9359639311; email: Ghanbari.env@gmail.com*

Received 29 March 2014; Accepted 22 November 2014

ABSTRACT

Feasibility of RSM-optimized electrocoagulation (EC) sludge recycling was studied in photo-Fenton (PF) process for the removal of Direct Blue 71. By EC process, relatively complete decolorization was obtained in pH 8, 20 min, and 150 mA. The produced sludge, in EC process, was evaluated to be used and recycled in PF process experimental runs for two major targets: (1) Degradation of EC sludge as an environmental, concerning by-product; (2) Application of iron species resulted from anodic dissolution during EC process to play the role of catalyst in PF process. PF process was investigated based on the effects of EC sludge volume (total iron) and hydrogen peroxide concentration on decolorization. Besides, the effect of EC sludge recycling on decolorization and mineralization (TOC decrement) was studied. In optimum conditions of PF process (pH 3, 200 mg/L H_2O_2, 20 mL EC sludge and 30 min reaction time in the first run), 96.27% decolorization was achieved. In the same conditions, but in 10 min, 67.5% TOC removal was obtained.

Keywords: Electrocoagulation; Sludge recycling; Direct Blue 71; Photo-Fenton

1. Introduction

Amongst environmental pollutants, dyes are one of the persistent ones posing significant pollution to the environmental compartments including water bodies. It is estimated that around 1–20% of the total azo dyes are lost during dying process entering the environment through wastewater discharge, particularly from the textile industries [1]. Textile wastewaters exhibit low BOD to COD ratios indicating the non-biodegradable nature of them [2]. Actually, the aromatic rings in the azo dye molecular structures make it toxic and mostly non-biodegradable; therefore, necessitating the application of vigorous separating/oxidative processes to overcome the separation/degradation of such persistent compounds [1,3,4]. Disappearance of color can occur if the colored dye molecule is precipitated and separated from the solution (coagulation). Color also disappears if the molecule is cleaved through oxidation reactions, by which the conjugated structure that absorbs visible wavelengths and thereby creates color is broken up.

*Corresponding author.

Electrocoagulation (EC) process is a separating process which has been successfully used for the treatment of textile wastewater [1,2] being attractive for its versatility, safety, selectivity, amenability to automation, ease of control, and environmental compatibility [2,5]. It mainly involves the generation of coagulant *in situ* by dissolution of metal ions from the consumable anode with simultaneous formation of hydroxide ions at the cathode. The electrochemical reactions occurring within an EC cell are summarized as given below [1,6,7]:
At the anode:

$$M \rightarrow M^{n+} + ne^- \quad (1)$$

$$2H_2O \rightarrow 4H^+ + O_2 + 4e^- \quad (2)$$

At the cathode:

$$2H_2O + 2e^- \rightarrow H_2 + 2OH^- \quad (3)$$

Regarding these Eqs. (1–3), the electro-generated metal ions (M^{n+}) immediately undergo further spontaneous reactions producing corresponding hydroxides and/or polyhydroxides having strong affinity for dispersed particles as well as counter ions bringing about the coagulation [1]. Meanwhile, the electro-generated gases including hydrogen and oxygen (mainly hydrogen), impinge the particles and coagulant aggregates upward, accelerating collisions between particles and coagulant by inducing more mixing [8]. Finally, the flocculated pollutants become separated either to the top or bottom of the EC cell depending on the dominant separation mechanism [9].

Although EC process provides remarkable separation efficiency, pollutants are not degraded considerably and are concentrated within the EC sludge. As a by-product, sludge brings about significant environmental nuisances imposing noticeable operational costs of handling and disposal [10]. Considering noticeable concentration of the flocculated pollutants, such sludge cries out for handling and disposal to comply with the environmental regulations. Apart from that, iron species in EC process sludge as a result of anodic dissolution are capable of acting as catalyst in some other processes. Fenton-based processes (Fenton, electro-Fenton, photo-Fenton (PF), and sono-Fenton) are viable processes in which iron plays the role of catalyst and reacts with hydrogen peroxide to form the strong destructive agent; the hydroxyl radical [11–13]. Initially, decomposition of hydrogen peroxide by the catalytic function of iron in acidic pH brings about the generation of hydroxyl radical (Fenton reaction) [14–17]:

$$Fe^{2+} + H_2O_2 \rightarrow Fe^{3+} + HO^{\cdot} + OH^- \quad (4)$$

Besides, in PF reaction, which is a viable Fenton configuration, hydroxyl radical is produced through the photolysis of hydrogen peroxide [18]:

$$H_2O_2 + UV \rightarrow HO^{\cdot} + HO^{\cdot} \quad (5)$$

In PF, UV radiation enhances pollutants degradation via generating additional hydroxyl radicals [19]. Likewise, based on equation 6, oxidized ferrous ion (Fe^{3+}) is photo-reduced back to the ferrous ion which reacts with hydrogen peroxide thereby resuming the hydroxyl radical generation cycle [12]. Indeed, regeneration of Fe^{2+} is accelerated via photo-reduction in PF when compared with the "simple" Fenton's process [20].

$$Fe^{3+} + UV + H_2O \rightarrow HO^{\cdot} + Fe^{2+} + H^+ \quad (6)$$

In this study, EC process with iron anodes was applied for efficient separation of Direct Blue 71 (DB71). The EC experiments were designed using response surface method (RSM). In a completely separate setup, PF process was conducted. In this way, in optimum condition of the EC process, sludge which contained iron species was separated and applied in the PF process for the bilateral target of agglomerated dye/sludge degradation along with providing iron source as a catalyst in the PF process. PF process was optimized; EC sludge along with the produced PF sludge was recycled several times in PF runs until no sludge was remained. Hence, sludge as a concerning environmental problem was degraded and at the same time, enhanced pollutant degradation. Accordingly, sludge produced in EC and PF experimental runs is used at source of production, waste minimization is obtained at source, and catalyst is used in place of reagents. These three advantages are among the green chemistry principles [21] which endorse the current study. The decrement of organic content of PF-treated samples was investigated through TOC analysis. Finally, PF process efficiency was evaluated in the presence and absence of EC sludge, UV, and hydrogen peroxide. In other words, four separate processes including PF (UV/H_2O_2/EC sludge), Fenton (H_2O_2/EC sludge), UV/H_2O_2, and photolysis with UV were carried out and compared based on the achieved decolorization efficiencies.

2. Materials and methods

2.1. Sample and reagents

DB71 dye ($C_{40}H_{23}N_7Na_4O_{13}S_4$) was supplied from Alvan Sabet company (Iran) with a purity of over 99% (CAS No. 4399-55-7, MW = 1029.9 g mol^{-1}, C.I. No. 34140). The chemical structure of DB71 is illustrated in Fig. 1. Samples were synthetically prepared with initial concentration of 100 mg/L DB71 for both EC and PF processes. All chemicals including sodium sulfate, sodium phosphate, sodium chloride, sodium nitrite, hydrogen peroxide, sulfuric acid, and sodium hydroxide were of analytical grade and obtained from the Merck Company.

2.2. EC setup and experiments

The EC process was conducted at room temperature in a rectangular glass-made reactor with dimensions of 11 × 5 × 14 cm and volume of 770 mL which was loaded with 600 mL electrolyte. Four iron sheets were used as cathodes and anodes having dimensions of 15 × 3 cm with total effective surface area of 144 cm^2. In order to power supply the EC system, a digital DC source (Zhaoxin, 0-2 A, and 0-20 V) was employed. Average voltage was recorded throughout the experiments for energy consumption calculation. Since dye samples were synthetically prepared using distilled water, sodium sulfate, sodium phosphate, sodium chloride, and sodium nitrite were separately added to the samples as supporting electrolytes to provide enough dissolved solids content thereby inducing electrical conductivity within the electrolyte. Solution pH was adjusted by adding certain amount of either 0.01 M sulfuric acid or 0.01 M sodium hydroxide. A magnetic stirrer was also used to agitate the electrolyte thoroughly. Samples were taken from the reactor within desired reaction times and filtered through 0.45 micron Whatman filter paper for absorbance measurement.

2.2.1. Design of experiment

EC process was designed using RSM. RSM is a technique for design of experiments that quantifies relationships among measured responses (dependent variables) and a number of input factors (independent variables). It is mainly used to find a combination of values for factors by which the optimal value of response is obtained. By this technique, much more precise evaluation is provided with much less number of experimental runs in comparison with rather conventional, time-consuming one-factor-at-a-time methods [22]. In this study, effects of factors including initial pH, electrical current (mA)/current density (mA cm^{-2}), and electrolysis time (min) on decolorization efficiency were evaluated using full central composite design (CCD) which is the most popular response surface design. The experimental runs were conducted in a randomized manner to minimize systematic bias. Data were analyzed using Minitab 16 software. Experimental points attributed to the independent variables were set as presented in Table 1. Eight star points ($\alpha = \pm 1$), six axial points ($\alpha = \pm 1.68$), and six replicates at the center point ($\alpha = 0$) were selected as experimental points.

2.3. PF process

Since anode electrodes in EC process were made of iron, EC sludge contained iron species which were supposed to be used as catalyst in the PF process. In this way, in optimal condition of EC process, solution pH was elevated to 9 to transform all iron species to non-soluble ones. Afterward, the whole electrolyte was centrifuged at 1,000 rpm for 15 min for the separation

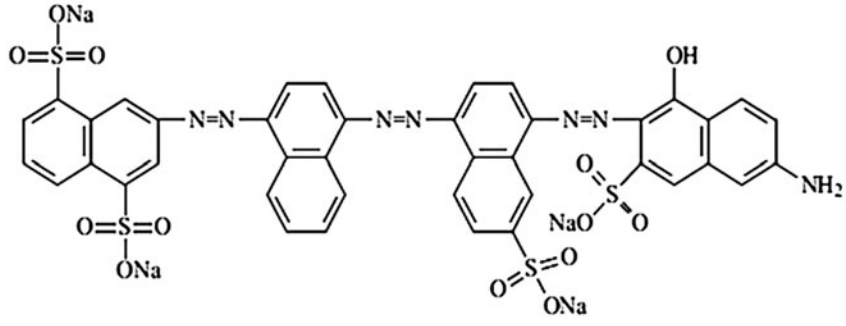

Fig. 1. Chemical structure of DB71.

Table 1
Coded and actual levels of independent variables

Coded levels					
Independent variables	−1.68	−1	0	+1	+1.68
Actual levels					
pH	5.3	6	7	8	8.7
Electrical current (mA)	66	100	150	200	234
Reaction time (min)	3	10	20	30	37

of sludge from the bulk solution. Then the supernatant was carefully decanted and the precipitated sludge was transferred to a storage container. Total volume of the EC sludge was about 60 mL. In the PF process, a cylindrical quartz reactor was loaded with 200 mL DB71 solution of 100 mg/L. Afterwards, centrifuged EC sludge was added to the dye solution. Then solution pH was adjusted to 3 using a pH glass electrode (WTW 720) calibrated with standard buffers at pH values of 4 and 7. Hydrogen peroxide was also added in three various concentrations to identify the appropriate ratio of EC sludge/H_2O_2. A 4 W UVC lamp (Philips®, 254 nm) was employed to provide the photolysis source of the PF process being installed on the outer wall of the quartz reactor facing the dye solution. The light intensity of the lamp was 9.5 W m^{-2}. By switching the UVC lamp on, the PF reactions were started. Magnetic stirrer was used to mix the solution thoroughly. Meanwhile, aliquots of 10 mL were taken in determined reaction times for immediate analysis. At the end of each PF run, whole reactor content, as well as the withdrawn samples, was centrifuged at 1,000 rpm for 15 min after elevating the pH up to 9. Then the separated sludge was wholly recycled in the next PF runs until complete degradation of sludge was accomplished and no sludge was remained in the PF reactor. The targets solved the problem of sludge and supplied iron from it. For the measurement of total organic carbon, samples were quenched with sodium nitrite and then analyzed by TOC analyzer.

2.4. Analyses

Decolorization efficiency was determined through measuring absorbance of filtered samples at $\lambda_{max} = 587$ nm which is the wavelength of maximum absorbance for DB71. Besides, absorbance within region between 200 and 700 nm was scanned. Absorbance measurements were carried out using Hach DR5000 UV–vis spectrophotometer.

TOC analysis was also conducted using TOC analyzer (Shimadzu; model TOC-VCHS, Japan). Total iron concentration was measured based on the corresponding procedure in the standard methods [23].

3. Results and discussion

3.1. Electrocoagulation

3.1.1. First step: selection of supporting electrolyte and electrode arrangement

In order to minimize the number of experimental runs in EC process and focus on more critical independent variables, EC was initially conducted under similar pH and electrical current (pH 8, 150 mA) to select appropriate supporting electrolyte and electrode arrangement. Four various supporting electrolytes with similar concentration of 5 mM were employed and the results are depicted in Fig. 2(a). Accordingly, the highest and the lowest decolorization efficiencies were obtained in the presence of sodium sulfate and sodium phosphate, respectively. Besides, sodium sulfate provided significantly higher decolorization within much shorter reaction time in comparison with the rest of the supporting electrolytes. Afterward, the effect of electrode arrangement was assessed in three different arrangements. As demonstrated in Fig. 2(b), high decolorization was achieved in short electrolysis time when electrodes were arranged in monopolar configuration. Hence, sodium sulfate and monopolar arrangement were selected and applied for the rest of the experiments.

3.1.2. EC process design of experiments

EC process was designed considering decolorization efficiency as the response. In this way, response surface analysis was employed to determine the experimental conditions. Three factors including pH, electrical current, and reaction time were considered. Eight star points ($\alpha = \pm 1.68$), six replicates at the center point ($\alpha = 0$), and 6 axial points were selected as experimental points. As presented in Table 2, 20 experimental runs were prescribed based on full CCD. The experimental and predicted values of the responses are also represented in Table 2.

RSM designs are capable of fitting a second-order prediction equation for the response [22]. In this way, the correlation of dependent variables and decolorization efficiency are revealed by the quadratic (second-order) polynomial response surface model which, in the general equation, is as follows:

$$Y = b_0 + \sum_{i=1}^{n} (b_i x_i) + \sum_{i=1}^{n} \left(b_{ii} x_{ii}^2\right) + \sum_{i,j=1}^{n} \left(b_{ij} x_i x_j\right) \quad (7)$$

where Y is the predicted response, b_0 is a constant, x_i represents the coded levels of independent variables,

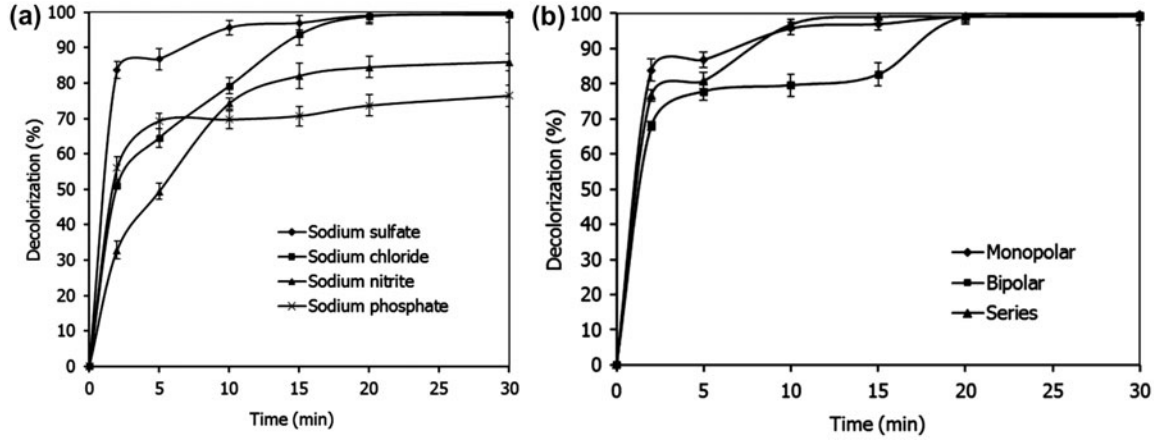

Fig. 2. (a) Effect of various supporting electrolytes (5 mM) on decolorization (pH 8, 150 mA, monopolar arrangement) and (b) Effect of electrode arrangement (pH 8, 150 mA, sodium sulfate used as supporting electrolyte).

Table 2
RSM design, experimental, and ANOVA-predicted values of the responses

	Actual levels of independent variables			Decolorization (%)	
Exp. runs	pH	Time (min)	E current (mA)	Experimental	Predicted
1	8	10	200	73.14	75.18
2	7	20	66	65	76.38
3	7	37	150	98.36	94.56
4	7	20	234	98	89.27
5	7	3	150	35.06	41.52
6	6	10	200	65.80	66.02
7	7	20	150	99.54	98.70
8	6	30	100	97	93.08
9	5.3	20	150	91.30	91.51
10	8	30	100	97.96	95.86
11	8	10	100	73.31	64.13
12	7	20	150	97.30	98.70
13	7	20	150	99.10	98.70
14	7	20	150	99.39	98.70
15	6	30	200	90.07	97.36
16	8	30	200	99.11	102.70
17	8.7	20	150	99.11	101.55
18	7	20	150	98.41	98.70
19	7	20	150	98.93	98.70
20	6	10	100	63	57.52

b_i, b_{ii}, and b_{ij} are the regression coefficients which stand for linear, quadratic, and interaction effects, respectively.

Based on the general quadratic response surface model, the following empirical relationship was obtained for the modeling of decolorization efficiency regarding various levels of the factors:

$$Y = 99.4625 + 2.9864X_1 + 15.7685X_2 + 3.8332X_3 - 1.0258X_1^2 - 11.1003X_2^2 - 5.8713X_3^2 - 0.9563X_1X_2 + 0.6388X_1X_3 - 1.0513X_2X_3 \quad (8)$$

In this equation, X_1, X_2, and X_3 represent pH, electrolysis time, and electrical current, respectively. Fig. 3

demonstrates the comparison of predicted and experimental decolorization.

High value of determination coefficient of 0.9633 endorses the validity of the corresponded quadratic polynomial equation (Eq. (8)). In other words, it confirms that the experimental values are in good agreement with the predicted values of the responses. Likewise, the adjusted R^2 which accounts for the number of parameters fit by the regression is 0.8979.

Parameter-estimated values and *t*-test distribution components are presented in Table 3. Actually, *p*-value and *t*-value demonstrate the significance of the coefficient. In this way, larger *t*-value along with smaller *p*-value indicates that the parameter is of higher significance [24]. In Table 3, regarding the estimations for b_1, b_2, and b_3, it is revealed that the highest and the lowest estimations corresponded to the coefficients of electrolysis time and pH, respectively. Likewise, highest *t*-value and lowest *p*-value are attributed to the electrolysis time. On this basis, electrolysis time has had the most significant influence on decolorization efficiency (with *p*-value of 0.000 and *t*-value of 8.45). This is also expectable because the dose of iron released from the anode increases by increase in electrolysis time, based on the Faraday's law [25]. Statistically, coefficients having *p*-value ≤ 0.05 are significant. Accordingly, the term electrolysis time with a *p*-value of 0.06 is quite a significant term. Amongst the quadratic coefficients, electrolysis time × electrolysis time and electrical current × electrical current were the significant terms. None of interaction terms were of significance.

Table 4 demonstrates the results of ANOVA for the first response; decolorization efficiency. The significance and adequacy of the model are supposed to be evaluated using analysis of variance [22].

The effects of factors including pH, reaction time, and electrical current on decolorization efficiency were evaluated, and the results are illustrated in Fig. 4. The response surface and contour plots illustrate the mutual interactions of two independent variables on the response. As illustrated in Fig. 4, each plot shows the interactive effects of two independent factors on the decolorization efficiency. In Fig. 4, the correlations of pH and electrolysis time on decolorization efficiency are revealed. It can be seen that decolorization efficiency is enhanced in higher levels of pH and time. This is supposed to be due to higher generation of hydroxide ions which are essential to cooperate and bond with the coagulant agents released from the anode to form an adsorptive surface for floc formation [26]. Besides, it has been stated that high pH levels decrease the zeta potential thereby enhancing the mutual collision between particles and bringing about higher EC efficiency [27]. Additionally, decolorization efficiency increases with time because of increase in concentration of coagulants and floc formation. Decolorization reached its optimum level in 20 min electrolysis since further increase in time didn't induce higher efficiency.

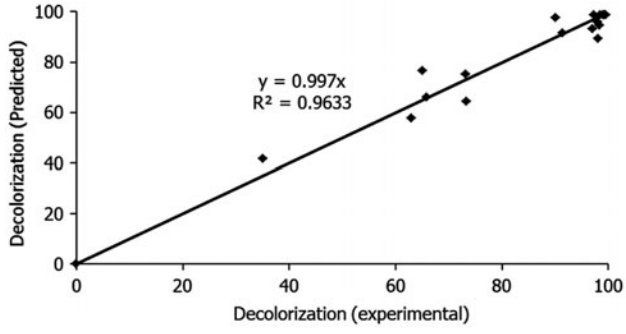

Fig. 3. Comparison of experimental and predicted values of response (decolorization).

Electrical current is another critical factor in the EC process which, its simultaneous effect with pH on decolorization, is depicted in Fig. 4. The current density values attributed to 66, 100, 150, 200, and 234 mA are 0.46, 0.69, 1.04, 1.39, and 1.62 mA cm^{-2}, respectively. Generally, increase in pH and electrical current enhances the decolorization efficiency. According to the Faradays law, dissolution of electrode is related to the total charge passed through it [28]. In other words, electrical current in higher levels increases metallic dissolution thereby inducing more coagulant species release into the electrolyte. At the same time, higher electrochemical reduction at the cathode creates more hydrogen bubbles which in turn, increase the collisions [26]. Nevertheless, electrical current over 200 mA resulted in lower efficiency. According to Fig. 4, it can be confirmed that the optimum electrical current and electrolysis time are 150 mA (current density of 1.04 mA cm^{-2}) and 20 min, respectively.

3.1.3. Optimum condition of the EC process

EC process was optimized based on the condition under which the highest decolorization efficiency is achievable experimentally. The highest decolorization efficiency was 99.54% which was obtained in optimum condition presented in Table 5.

Electrical energy consumption is of high concern within all electrochemical processes and is commonly calculated through the following equation [17]:

Table 3
Estimated regression coefficients for decolorization efficiency

Coefficient	Parameter estimate	Standard deviation	*t*-value	*p*-value	Significance
b_0	99.4625	2.805	35.463	0.000	–
b_1	2.9864	1.861	1.605	0.140	Non-significant
b_2	15.7685	1.861	8.474	0.000	Significant
b_3	3.8332	1.861	2.060	0.066	Significant
b_{12}	−0.9563	2.431	−0.393	0.702	Non-significant
b_{13}	0.6388	2.431	0.263	0.798	Non-significant
b_{23}	−1.0513	2.431	−0.432	0.675	Non-significant
b_{11}	−1.0258	1.811	−0.566	0.584	Non-significant
b_{22}	−11.1003	1.811	−6.128	0.000	Significant
b_{33}	−5.8713	1.811	−3.241	0.009	Significant

Table 4
ANOVA table for decolorization efficiency

Source	Sum of squares	Degree of freedom	Mean square	*F*-value
Regression	5,848.12	9	649.79	13.74
Residual error	472.90	10	47.29	
Total	6,321.02	19		

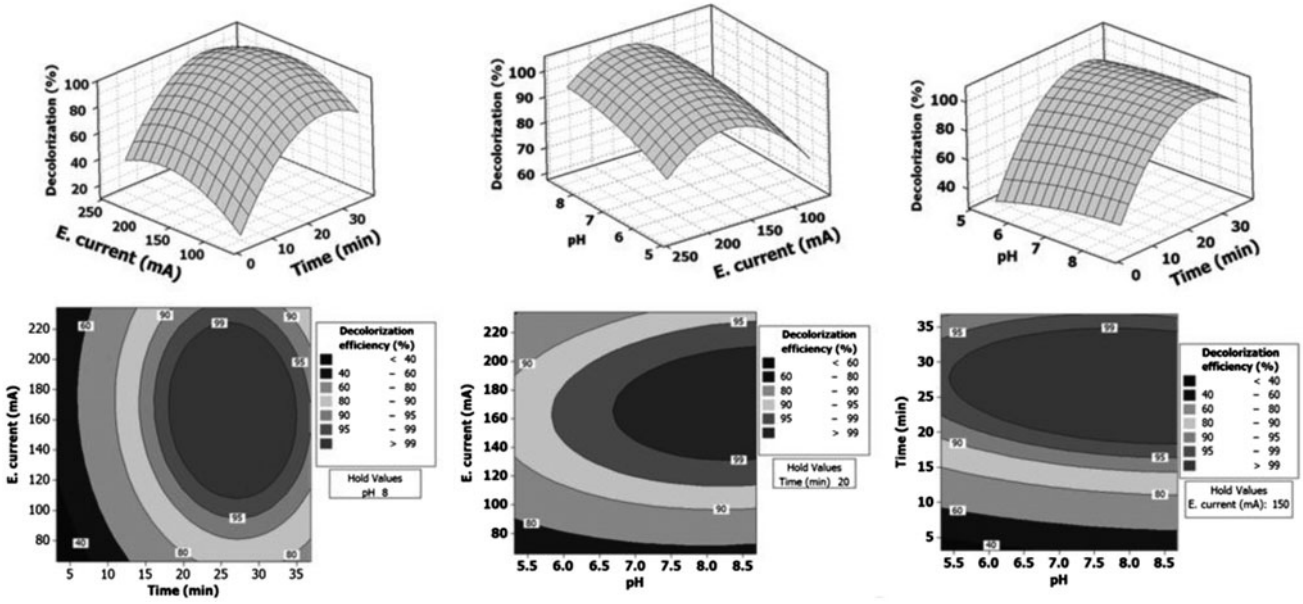

Fig. 4. Response surface and contour plots of decolorization as a function of pH, electrical current (mA), and reaction time (min).

$$E = \frac{UIt}{1000} \quad (9)$$

where E is the electrical energy consumption (kWh), U is the applied voltage (volt), I is the electrical current (A), and t is the reaction time (h).

Accordingly, the electrical energy consumption needed for optimum decolorization of $1\,m^3$ studied wastewater using EC process is 0.4 kWh. Likewise, the electrical energy consumption for the removal of $1\,kg\,m^{-3}$ DB71 in optimum condition is 2.4×10^{-3} kWh.

Table 5
Optimum conditions of EC process

Parameter	Value
pH	8
Electrolysis time (min)	20
Electrical current (mA)	150

3.2. PF process (dye decomposition as well as sludge reuse and degradation)

3.2.1. Effect of EC sludge volume (total iron)

Concentration of iron as the catalyst is a crucial factor in Fenton process [29]. As it was formerly described, iron species required to react with hydrogen peroxide to form hydroxyl radical was supplied by adding certain volume of EC sludge to the PF reactor. The effect of EC sludge amount (total iron concentration) on decolorization efficiency was investigated and the results are depicted in Fig. 5. As seen, by the addition of 15 mL EC sludge, decolorization efficiency is not considerable, and in its highest value reaches to about 36%. In the next run of PF, 20 mL EC sludge was applied yielding significantly high decolorization efficiency shortly after the reaction was started up (over 90% decolorization efficiency in 5 min reaction time). This is supposed to be attributed to higher generation of hydroxyl radical [30]. Afterwards, 25 mL EC sludge was used by which less decolorization rate resulted. These results are also in agreement with those reported within literatures where it has been stated that after an optimal concentration of Fe^{2+}, further increase in it exhibits negligible efficiency improvement or less efficiency due to adverse effect of excessive ferrous ion dosage [19,31]. Consequently, 20 mL EC sludge with a total iron of 27.7 ± 3 mg/L along with 200 mg/L H_2O_2 fulfilled the effective ratio of Fe/H_2O_2 to form the major degrading agent; the hydroxyl radical.

3.2.2. Effect of hydrogen peroxide concentration

To evaluate the effect of hydrogen peroxide concentration, three different concentrations were examined and the results are demonstrated in Fig. 6. As shown, by increasing the H_2O_2 concentration from 50 to 200 mg/L, decolorization efficiency is enhanced. Actually, it is expected that reasonably high concentrations of hydrogen peroxide increase generation of hydroxyl radical by which higher degradation occurs [20]. Accordingly, 200 mg/L hydrogen peroxide was found to be the most efficient concentration with decolorization efficiencies of over 90% during the reaction times reaching a maximum of 96.27% in 30 min reaction time. Further increase in H_2O_2 concentration was avoided since by 200 mg/L H_2O_2, the decolorization efficiency was satisfying (96.27%).

3.2.3. Effect of EC sludge recycling on decolorization by PF

In optimum conditions of the PF process (pH 3, 20 mL EC sludge, 200 mg/L H_2O_2), the recycling of the

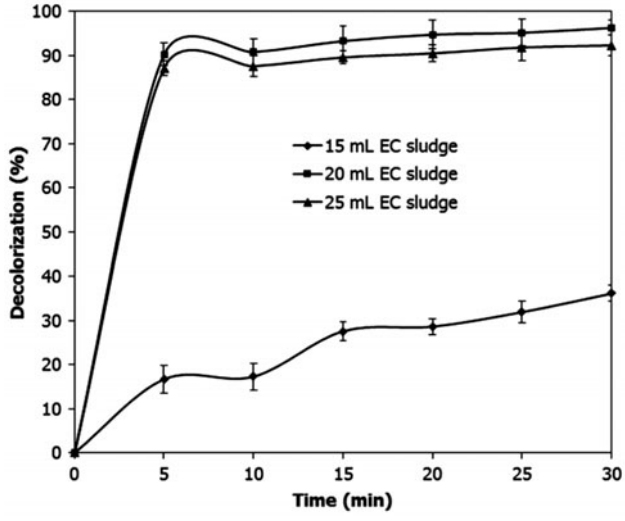

Fig. 5. The effect of EC sludge volume (total iron concentration) on decolorization efficiency (100 mg/L direct blue, pH 3, 200 mg/L H_2O_2).

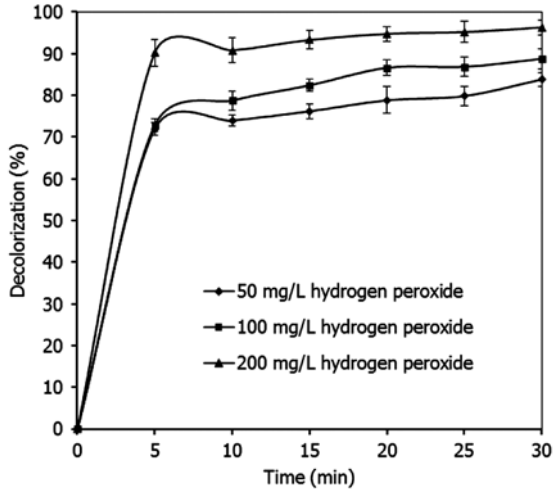

Fig. 6. Effect of hydrogen peroxide concentration on decolorization efficiency within various reaction times (pH 3, 20 mL EC sludge containing total iron of 27.7 ± 3 mg/L).

sludge was experimented in as much as achieving zero sludge production. On this basis, it took eight runs to completely degrade the recycling EC and PF sludge. It should also be noted that within all these eight PF runs, decolorization efficiency was over 75% (75–96%). As observed in Fig. 7, the highest decolorization was obtained in fresh sludge (run 1) especially at 5 min reaction time. The decolorization efficiencies at 5 min reaction time were in the range of 27.2–90.2% and corresponded to fresh sludge (run 1) and run 5, respectively. This difference in efficiency can be attributed to the amount of iron dissolved in solution at former runs and decrease in iron at sludge for further experiments consequently. In addition, reaction rate in the presence of fresh EC sludge (run 1) is higher than those of the rests. Furthermore, decolorization efficiencies at 30 min reaction time were close to each other in all runs (74–96%). These results might be related to less organic load-driven sludge degradation in former runs. Despite different efficiencies in run 5 (having the lowest efficiency) in comparison with those of other runs are not understood, further studies are required for justification of this phenomenon.

3.2.4. Effect of EC sludge recycling on mineralization by PF

During oxidative decolorization of dye solution, hydroxyl radical as the major degrading agent, mostly and essentially decomposes the azo agent in a dye structure [32]. This leads to the decrement in absorbance within wavelength of maximum absorbance of dye determined as decolorization. But apart from it, intermediate substances are also a consequence of dye defragmentation where their occurrence and degradation are not visible. In order to assess the mineralization rate in eight runs of PF with sludge recycling to supply iron, TOC analysis was carried out. As it was formerly seen in Fig. 7, decolorization rates in almost all eight runs of PF were remarkable within 10 min revealing high reaction rate in this reaction time in which the major portion of decolorization was accomplished. For this reason, TOC analysis was performed for aliquots which were withdrawn in 10 min reaction time, and the results are shown in Fig. 8. As can be observed, TOC removal is in its highest level in the first run and with a negligible decrement, in the third one, both exhibiting over 65% TOC removal efficiency. On the other hand, the lowest TOC removal belongs to the second run. Generally, despite the recycling of the sludge which contains complex mixture of organic and mineralized compounds, TOC removal efficiencies of these eight runs are somehow close to each other ranging between 51 and 67%; which can be interpreted as a positive and justifying point in sludge recycling within PF experimental runs.

3.2.5. Spectral changes investigation for possible destructive reactions

Light absorbance scan is a valuable method to recognize absorbance variations in high absorption solutions specially those containing dyes. In this way, initial sample containing 100 mg/L DB71 and effluents

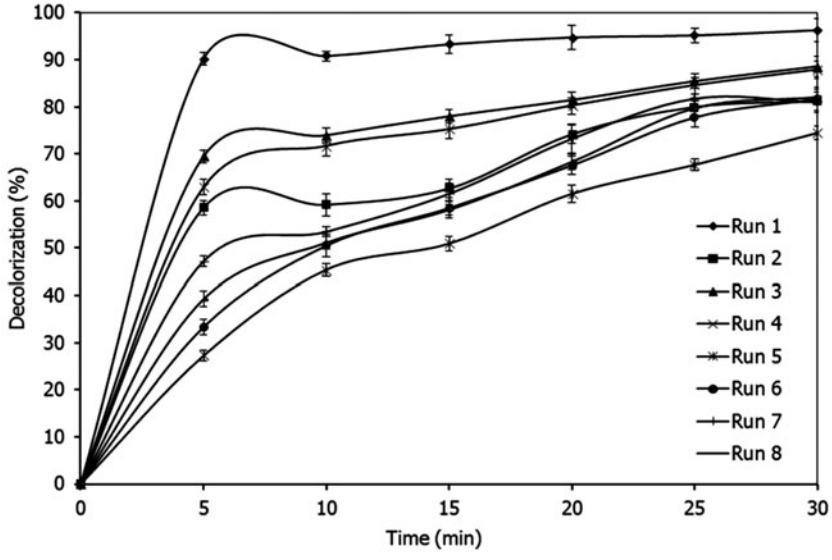

Fig. 7. Decolorization efficiency in eight stages of sludge recycling in PF process (pH 3, H_2O_2 = 200 mg/L).

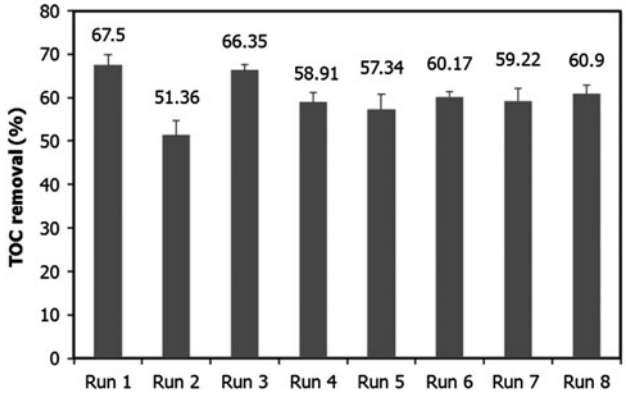

Fig. 8. TOC analysis in PF process (pH 3, 200 mg/L H_2O_2, 20 mL EC sludge, 10 min reaction time).

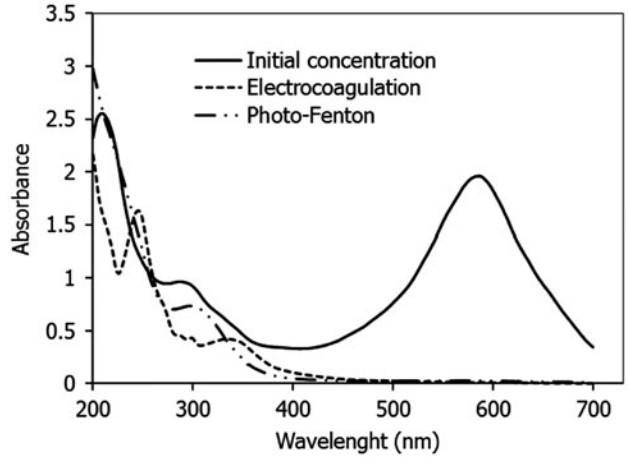

Fig. 9. Wavelength scan of initial dye sample (100 mg/L), EC effluent in optimized conditions (pH 8, 20 min electrolysis, 150 mA), PF effluent in optimized conditions (pH 3, 30 min reaction time, 200 mg/L H_2O_2).

of EC and PF processes in optimum conditions were scanned separately to investigate absorbance variations within the spectrum of 200–700 nm. As can be seen in Fig. 9, the wavelength in which maximum absorbance of DB71 is observed is 587 nm. On this basis, UV absorbance of EC and PF effluents at 587 nm is supposed to be a suitable index which has been decreased significantly to around an absorbance of zero which endorses over 95% decolorization by these two processes. Considering the absorbance variations of the initial DB71 solution, two major peaks can be observed at 210 nm and 290 nm which correspond to benzene and naphthalene rings in DB71 structure, respectively. On this basis, benzene and naphthalene removal mostly occurred by the EC process. On the other hand, it cannot be stated that PF process is not generally efficient in benzene and naphthalene removal since within PF, EC sludge was recycled and, in turn, increased the absorbance in these two wavelengths as it was definitely expected. Nevertheless, absorbance decrease at 587 nm (decolorization) in both EC and PF processes are quite equal. The reason might be explained as follows: in PF process, decolorization stems from conversion of $n \rightarrow \pi^*$ which is much easier for the hydroxyl radical in comparison to the conversion of $\pi \rightarrow \pi^*$ [29,32].

3.2.6. Comparison (PF, Fenton, UV/H_2O_2, and UV)

Four separate processes were conducted to reveal the decomposing capabilities of UV, total iron, and hydrogen peroxide independently and the corresponding results are shown in Fig. 10. As shown, the highest decolorization is attributed to the PF process in which all three agents (total iron, H_2O_2, and UV) are exerted. In this process, over 90% decolorization is gained within 5 min of reaction time exhibiting a significant decolorization rate. The next process was carried out in the absence of UV, in which hydrogen peroxide and total iron (EC sludge) were applied to form hydroxyl radical in the Fenton process. Decolorization trend in Fenton process is quite similar to that of the PF process, while the reaction rate of Fenton process is much less in comparison with that of the PF process. Thus, UV has definitely enhanced the decolorization in PF process. It is supposed to be due to more generation of hydroxyl radical in PF process. The next process was carried out to investigate the capability of EC sludge as a source of total iron used in PF and

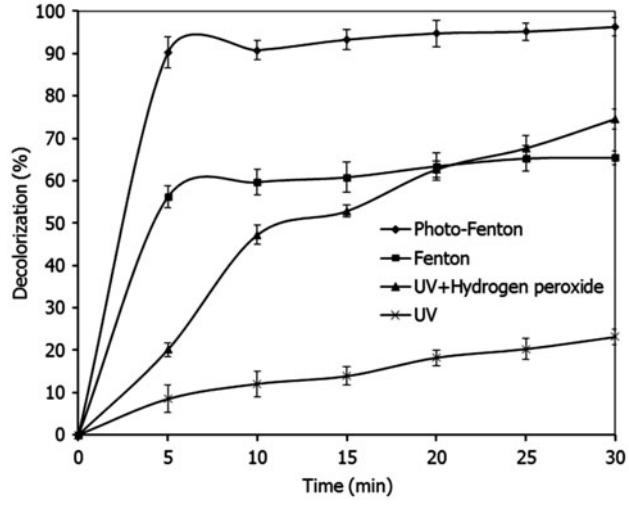

Fig. 10. Comparison of decolorization efficiency in four different processes in optimized conditions (pH 3, 200 mg/L H_2O_2, 20 ml EC sludge).

Fenton processes. To do this, experiments were conducted in the presence of UV and hydrogen peroxide by which over 70% decolorization efficiency was obtained in 30 min. It should also be noted that in absence of EC sludge (total iron), reaction rate is considerably lower, while in presence of it (in PF and Fenton processes) a sharp decolorization rate is conspicuous. Finally, UV as the only employed degradation agent yields negligible decolorization efficiency (about 23% decolorization efficiency in 30 min).

4. Conclusions

EC process was optimized for the removal of DB71. The optimum condition was pH 8, 150 mA, and 20 min electrolysis by which 99.54% decolorization was obtained with 2.4×10^{-3} kWh (kg m^{-3} removed dye)$^{-1}$ energy consumption. The produced sludge in EC process was recycled in PF process for degradation of sludge and also using total iron as catalyst. In optimum condition of pH 3, 200 mg/L hydrogen peroxide, and 20 mL EC sludge, 96.27% decolorization was obtained in the first PF run. Sludge produced in EC and PF processes was recycled in eight runs until no sludge was produced. Furthermore, 67.5% TOC removal was achieved in pH 3, 200 mg/L H_2O_2, and 10 min. It is concluded that iron species in EC sludge are capable of acting as catalyst in Fenton-based processes followed by solving the problem of sludge handling and disposal.

Acknowledgments

We are grateful to the authorities of Alvan Sabet Company where the studied dye was purchased from. We are also grateful to the anonymous reviewers for their invaluable comments on the previous version of this manuscript.

References

[1] C. Thakur, V.C. Srivastava, I.D. Mall, Electrochemical treatment of a distillery wastewater: Parametric and residue disposal study, Chem. Eng. J. 148 (2009) 496–505.
[2] G. Mouedhen, M. Feki, M.D.P. Wery, H.F. Ayedi, Behavior of aluminum electrodes in electrocoagulation process, J. Hazard. Mater. 150 (2008) 124–135.
[3] M.S. Secula, B. Cagnon, T.F. de Oliveira, O. Chedeville, H. Fauduet, Removal of acid dye from aqueous solutions by electrocoagulation/GAC adsorption coupling: Kinetics and electrical operating costs, J. Taiwan Inst. Chem. Eng. 43 (2012) 767–775.
[4] T. Zhou, X. Lu, J. Wang, F.-S. Wong, Y. Li, Rapid decolorization and mineralization of simulated textile wastewater in a heterogeneous Fenton like system with/without external energy, J. Hazard. Mater. 165 (2009) 193–199.
[5] N. Modirshahla, M.A. Behnajady, S. Mohammadi-Aghdam, Investigation of the effect of different electrodes and their connections on the removal efficiency of 4-nitrophenol from aqueous solution by electrocoagulation, J. Hazard. Mater. 154 (2008) 778–786.
[6] W. Balla, A.H. Essadki, B. Gourich, A. Dassaa, H. Chenik, M. Azzi, Electrocoagulation/electroflotation of reactive, disperse and mixture dyes in an external-loop airlift reactor, J. Hazard. Mater. 184 (2010) 710–716.
[7] F. Ghanbari, M. Moradi, A. Eslami, M.M. Emamjomeh, Electrocoagulation/flotation of textile wastewater with simultaneous application of aluminum and iron as anode, Environ. Processes 1 (2014) 447–457.
[8] D. Valero, J.M. Ortiz, V. García, E. Expósito, V. Montiel, A. Aldaz, Electrocoagulation of wastewater from almond industry, Chemosphere 84 (2011) 1290–1295.
[9] P.K. Holt, G.W. Barton, C.A. Mitchell, The future for electrocoagulation as a localised water treatment technology, Chemosphere 59 (2005) 355–367.
[10] Y. Cui, T. Sun, L. Zhao, T. Jiang, L. Zhang, Performance of wastewater sludge ecological stabilization, J. Environ. Sci. 20 (2008) 385–389.
[11] S. Figueroa, L. Vázquez, A. Alvarez-Gallegos, Decolorizing textile wastewater with Fenton's reagent electrogenerated with a solar photovoltaic cell, Water Res. 43 (2009) 283–294.
[12] A. Zapata, T. Velegraki, J.A. Sánchez-Pérez, D. Mantzavinos, M.I. Maldonado, S. Malato, Solar photo-Fenton treatment of pesticides in water: Effect of iron concentration on degradation and assessment of ecotoxicity and biodegradability, Appl. Catal. B 88 (2009) 448–454.
[13] F. Ghanbari, M. Moradi, M. Manshouri, Textile wastewater decolorization by zero valent iron activated peroxymonosulfate: Compared with zero valent copper, J. Environ. Chem. Eng. 2 (2014) 1846–1851.
[14] J. Herney-Ramirez, M.A. Vicente, L.M. Madeira, Heterogeneous photo-Fenton oxidation with pillared clay-based catalysts for wastewater treatment: A review, Appl. Catal. B 98 (2010) 10–26.
[15] J.J. Pignatello, E. Oliveros, A. MacKay, Advanced oxidation processes for organic contaminant destruction based on the Fenton reaction and related chemistry, Crit. Rev. Environ. Sci. Technol. 36 (2006) 1–84.
[16] S. Santos da Silva, O. Chiavone-Filho, E. Barros Neto, E. Foletto, A. Mota, Effect of inorganic salt mixtures on phenol mineralization by photo-Fenton-analysis via an experimental design, Water Air Soil Pollut. 225 (2013) 1–10.
[17] A. Eslami, M. Moradi, F. Ghanbari, F. Mehdipour, Decolorization and COD removal from real textile wastewater by chemical and electrochemical Fenton processes: A comparative study, J. Environ. Health Sci. Eng. 11 (2013) 1–8.
[18] A.N. Módenes, F.R. Espinoza-Quiñones, F.H. Borba, D.R. Manenti, Performance evaluation of an integrated photo-Fenton—electrocoagulation process applied to pollutant removal from tannery effluent in batch system, Chem. Eng. J. 197 (2012) 1–9.
[19] F. Ay, E.C. Catalkaya, F. Kargi, A statistical experiment design approach for advanced oxidation of

direct red azo-dye by photo-Fenton treatment, J. Hazard. Mater. 162 (2009) 230–236.
[20] T. Maezono, M. Tokumura, M. Sekine, Y. Kawase, Hydroxyl radical concentration profile in photo-Fenton oxidation process: Generation and consumption of hydroxyl radicals during the discoloration of azo-dye Orange II, Chemosphere 82 (2011) 1422–1430.
[21] L.H. Keith, L.U. Gron, J.L. Young, Green analytical methodologies, Chem. Rev. 107 (2007) 2695–2708.
[22] A.R. Khataee, M. Zarei, A.R. Khataee, Electrochemical treatment of dye solution by oxalate catalyzed photo-electro-Fenton process using a carbon nanotube-PTFE cathode: Optimization by central composite design, CLEAN - Soil, Air, Water 39 (2011) 482–490.
[23] APHA, Standard Methods for the Examination of Water and Wastewater, twentieth ed., APHA, Washington, DC, 1999.
[24] A.I. Khuri, J.A. Cornell, Response Surface: Design and Analysis, Marcel Dekker, New York, 1987.
[25] F. Ghanbari, M. Moradi, A. Mohseni-Bandpei, F. Gohari, T. Mirtaleb Abkenar, E. Aghayani, Simultaneous application of iron and aluminum anodes for nitrate removal: A comprehensive parametric study, Int. J. Environ. Sci. Technol. 11 (2014) 1653–1660.
[26] G. Chen, Electrochemical technologies in wastewater treatment, Sep. Purif. Technol. 38 (2004) 11–41.
[27] P.K. Holt, G.W. Barton, M. Wark, C.A. Mitchell, A quantitative comparison between chemical dosing and electrocoagulation, Colloids Surf. A 211 (2002) 233–248.
[28] P. Ratna Kumar, S. Chaudhari, K.C. Khilar, S.P. Mahajan, Removal of arsenic from water by electrocoagulation, Chemosphere 55 (2004) 1245–1252.
[29] P.A. Carneiro, R.F.P. Nogueira, M.V.B. Zanoni, Homogeneous photodegradation of C.I. reactive blue 4 using a photo-Fenton process under artificial and solar irradiation, Dyes Pigm. 74 (2007) 127–132.
[30] T.M. Elmorsi, Y.M. Riyad, Z.H. Mohamed, H.M.H. Abd El Bary, Decolorization of Mordant red 73 azo dye in water using H_2O_2/UV and photo-Fenton treatment, J. Hazard. Mater. 174 (2010) 352–358.
[31] M. Moradi, F. Ghanbari, Application of response surface method for coagulation process in leachate treatment as pretreatment for Fenton process: Biodegradability improvement, J. Water Proc. Eng. 4 (2014) 67–73.
[32] N. Ertugay, F.N. Acar, Removal of COD and color from Direct Blue 71 azo dye wastewater by Fenton's oxidation: Kinetic study. Arab. J. Chem. (2013). doi:10.1016/j.arabjc.2013.1002.1009.